Investigation of an opposed-contact GaAs photoconductive semiconductor switch at 1-kHz excitation

Xu, M.; Dong, H.; Liu, C.; Wang, Y.; Hu, L.; Lan, C.; Luo, W.; Schneider, H.;

Originally published:

March 2021

IEEE Transactions on Electron Devices 68(2021)5, 2355-2359

DOI: https://doi.org/10.1109/TED.2021.3066094

Investigation of an Opposed-Contact GaAs Photoconductive Semiconductor Switch at 1-kHz Excitation

Ming Xu, *Senior Member, IEEE*, Hangtian Dong, Chun Liu, Yi Wang, Long Hu, Chunpeng Lan, Wei Luo, and Harald Schneider

***Abstract*—The transient performance of gallium arsenide (GaAs) photoconductive semiconductor switches (PCSS) triggered by laser diodes (LD) at nano-joules (nJ) energy, is of great significance for the potential high-power applications at high repetition rates. An opposed-contact GaAs PCSS with Ni/AuGe/WTi/Au electrodes is presented at single-shot and 1-kHz excitation. The influences of bias electric field up to 80 kV/cm on nonlinear characteristics are investigated quantitatively with a carriers' avalanche multiplication factor as high as 0.8 ×10^4. The effect of electric field on the carriers' dynamic process and thermal accumulation in repetitive operation is analyzed. The transient electric field distribution is demonstrated by an ensemble Monte Carlo simulation.**

***Index Terms*—Gallium arsenide (GaAs), high gain, photoconductive semiconductor switch, avalanche, repetition rate**

I. Introduction

Optically triggered switches possess a number of advantages that include: the ultrafast rise time, high power delivery capacity, optical control and isolation, and module scalability [1]-[8]. Concerning the bandgap-dependent wavelength and optical excitation energy, which could add the complexity and system cost, PCSS based on semi-insulating (SI) GaAs material continue to be developed in the recent past [1]-[9]. In contrast to the linear mode of GaAs PCSS, the nonlinear or high-gain (HG) mode is characterized by five orders of magnitude reduction in the optical excitation energy. Consequently, a low optical energy especially in the nJ regime, is sufficient to excite the GaAs PCSS into HG mode. However, the bias electric field will increase dramatically as the optical excitation energy is reduced into the nJ range. For the targeted applications, an inexpensive LD for excitation is demanded which allows for the compact, palm-size dimension of the entire system. On the other hand, it is required that the PCSS can withstand a higher bias electric field to switch the stable transients at large repetition rates. However, the duration of the HG mode normally lasts for tens to hundreds of nanoseconds (ns), in which the current would produce enough heat to melt or anneal the contacts. In this regard, a different charging method, device geometry and electrode metallization have been explored to optimize the transient performance for non-destructive operation at high repetition rate [4], [6], [10].

In this article, we report our experimental optimization of an opposed-contact GaAs PCSS with Ni/AuGe/WTi/Au alloy electrodes for high gain repetitive photo switching using a LD. A pulse-forming line for pulsed-bias operation rather than a simple RC circuit is utilized, which reduces the heat accumulation at repetitive operation. The characteristics of single-shot and repetitive operation are investigated at nJ excitation, which allows one to gain an insight into the transient characteristics of HG operation at low optical excitation energy of nJ.

II. Experimental setup

An opposed-contact GaAs PCSS is used in our experiment, as shown in Fig. 1. The resistivity of SI GaAs is 5×10^7 Ω·cm in total darkness and the electron mobility is greater than 6000 cm^2/(V·s). The Ni/AuGe/WTi/Au (10 nm/ 200 nm/ 20 nm/ 200 nm) electrodes are deposited on the surface of the SI GaAs by electron-beam evaporation and annealed between 350 ºC and 400 ºC for 1 minute to form ohmic contacts [11]. The two electrodes have a horizontal spacing of 1 mm. Gold thermocompression wire bonding is implemented to preserve the bondpad layer, which can optimize the longevity of device. A 900 nm Si_3N_4 layer is deposited on the GaAs surface as the passivation layer. In this experiment, the GaAs PCSS is excited by a LD via a multimode fibre at a wavelength of 905 nm. The full width at half-maximum (FWHM) of the optical pulse is about 9 ns. The utilization of LD replacing the

This work was supported in part by the National Natural Science Foundation of China under Grant 51877177, Grant 51707162, and Grant 52007152, in part by the Scientific Research Program Funded by Shaanxi Provincial Education Department under Grant 19JC032 and the Youth Innovation Team of Shaanxi Universities, in part by the State Key Laboratory of Infrared Physics, Chinese Academy of Sciences under Grant M201919, in part by Open Research Fund of State Key Laboratory of Pulsed Power Laser Technology under Grant SKL2020KF01. (Corresponding author: Ming Xu and Long Hu)

M. Xu, H. Dong, C. Liu, Y. Wang, C. Lan and W. Luo are with the Department of Applied Physics, Xi'an University of Technology, Xi'an 710048, China (e-mail: xuming@xaut.edu.cn)

Long Hu is with Key Laboratory for Physical Electronics and Devices of the Ministry of Education, Xi'an Jiaotong University, Xi'an, 710049, China. (email: hulong_1226@hotmail.com)

Harald Schneider is with the Helmholtz-Zentrum Dresden-Rossendorf, Dresden 01328, Germany.

desktop laser can allow an extremely compact switching system in specific applications.

The switch is charged by a pulse-forming line (PFL) and the impedance is 50 Ω. The output pulse is recorded by an oscilloscope (LeCroy Wavemaster 8620 A, 20 GS/s) with a bandwidth of 6GHz via 10-60dB/4GHz/50Ω attenuators. A pulsed bias is measured by a probe (P6015A) with a bandwidth of 75 MHz. The LD driver and pulsed bias receive the command signals from a Stanford DG645 pulse generator to ensure the synchronous triggering of the PCSS with the pulse charger. The diameter and single-pulse energy of the laser beam are about 200 μm and ~140 nJ, respectively.

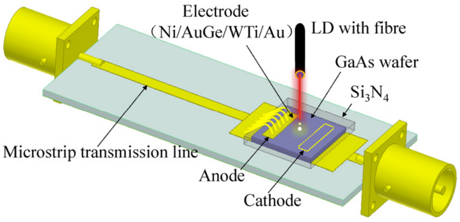

Fig. 1. Schematics of the nonlinear GaAs PCSS with opposed electrodes.

III. Results and Discussion

A. *Different switching characteristics at nJ excitation*

Normally, the maximum voltage that PCSS can sustain depends on the electrode gap size, which should be large enough to hold off the electric field strength. Furthermore, the flashover or breakdown can be controlled by increasing the gap between the contacts. On the other hand, for almost all HG GaAs PCSS in specific applications, it is required that the PCSS is optimized to achieve the reliable switching with minimum optical excitation energy. However, the laser energy required to generate a given conductance will increase quadratically with the gap distance. In our experiment, the bias electric field is increased from 0.88 kV/cm to 72 kV/cm while the optical excitation is maintained at 140 nJ. The switching waveforms for single-shot operation is shown in Fig. 2.

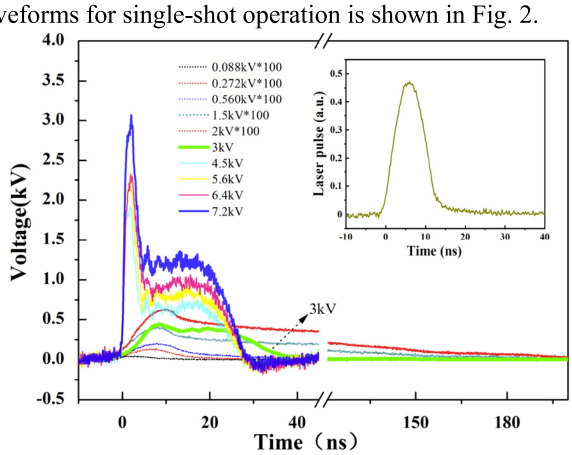

Fig.2. The switching waveforms for single-shot operation with respect to different bias voltages. The lower five traces are already enlarged by one hundred times for legibility.

It should be noted that the lower five waveforms (0.088 kV, 0.272 kV, 0.56 kV, 1.5 kV and 2.0 kV) are already enlarged by 100 times for the purpose of legibility. The inset is the optical pulse of LD and the FWHM is about 9 ns. Compared with the optical pulse, the waveforms appear in the form of the linear characteristics as the bias voltage increases to 0.56 kV, and the corresponding FWHM is also about 9 ns. When the bias voltage increases to 1.5 kV, the waveform starts to decay exponentially to 200 ns. It implies that the negative differential mobility (NDM) occurs in the GaAs PCSS. When the bias voltage increases to 3 kV, the waveform transforms to a shorter tail than that of 2 kV. The upper four waveforms (4.5 kV, 5.6 kV, 6.4 kV, and 7.2kV) at higher electric field are featured with a lock-on stage of 30 ns. These variable lock-on durations indicate that there exists a pulse compression process, following the increase of electric field. It is assumed that the transport of photogenerated carriers shifts to a different physical mechanism as the bias electric field increases further.

The HG GaAs PCSS can be operated at lower optical excitation than linear PCSS, which is attributed to two effects: carriers' avalanche multiplication and recombination compensation. In principle, the avalanche multiplication factor (*M*) in GaAs can be estimated as follows:

$$M = N / N_a \tag{1}$$

where N and N_a are the number of carriers which are created in total (i.e., by photon excitation and by impact ionization) and the number of carriers created by photon absorption, respectively. In practice, the number of carriers is equivalent to the integral area under the switching waveform, which is recorded by the oscilloscope. On the other hand, the absorbed photons can be estimated by the corresponding optical excitation energy. Certainly, if the quantum efficiency in photoconduction and the reflection of incident laser are considered, the number of absorbed photons will be lower.

Therefore, a relative avalanche multiplication factor can be demonstrated by the ratio of integral area under the waveform and the number of incident photons. As shown in Fig. 3, the electric field dependence of normalized *M* and the risetime are presented as the optical excitation is fixed at 140 nJ. It should be noted that the bias electric field is increased further to 80 kV/cm. There is no distinct difference of *M* as the bias electric field increases to 20 kV/cm (i.e., at 2 kV bias voltage). The value of *M* begins to raise distinctly as the electric field reaches at 30 kV/cm, which is increased by nearly four orders of magnitude and in good agreement with the description of waveforms variation in Fig.2.

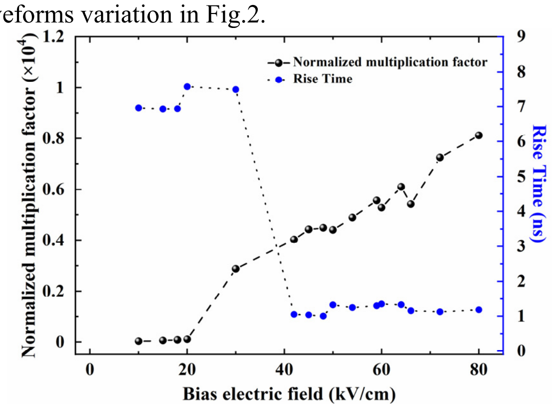

Fig.3. The normalized avalanche multiplication factor and experimental risetime with respect to the bias electric field (from 0.88kV/cm to 80 kV/cm) at 140 nJ excitation.

On the other hand, as the electric field is increased to 45 kV/cm, the risetime shows to be nearly seven times faster than that of 30 kV/cm. It is verified that there is a different photogenerated carriers' kinetic characteristic from 45 kV/cm to 80 kV/cm, in contrast to that of the lower electric field.

B. Electric field dependence of photogenerated carriers' dynamic process at nJ excitation

As we all know, the L and X valley minima are 0.31 eV and 0.36 eV above the Γ valley minimum in GaAs, respectively. The intervalley scattering will occur as the photogenerated carriers have sufficient energy in the electric bias field. Furthermore, the transfer of carrier will undergo from a high mobility energy valley to low mobility and high-energy satellite valleys. The average carrier drift velocity in GaAs PCSS can be expressed by [12]:

$$\overline{v}_d = (n_\Gamma v_{d\Gamma} + n_s v_{s\Gamma})/(n_\Gamma + n_s) \tag{2}$$

where n_Γ and n_s are the carrier's concentration in the Γ valley and the satellite valley, respectively, $v_{d\Gamma}$ and v_{ds} are the carrier velocity of the corresponding valleys. In low electric field, the $v_{d\Gamma}$ is much lower than v_{ds}, so the Eq. (2) can be simplified as:

$$\overline{v}_d = n_\Gamma v_{d\Gamma} / n \tag{3}$$

The carriers with higher energy start to transfer to the upper valleys and the amount of n_Γ will decease when the bias electric field increases higher. Considering the variation of n_Γ and $v_{d\Gamma}$ following the increase of the bias electric field, the derivative of the average carrier drift velocity with respect to the electric field can be expressed:

$$\frac{d\overline{v}_d}{dE} = \frac{1}{n}\left(n_\Gamma \frac{dv_{d\Gamma}}{dE} + v_{d\Gamma}\frac{dn_\Gamma}{dE}\right) \tag{4}$$

The negative differential mobility will occur as the decreasing of the amount of n_Γ can overcome the increase of $v_{d\Gamma}$. The average electron drift with respect to electric field at optical excitation can be demonstrated by an ensemble Monte Carlo (EMC) simulation, in which an 80 × 80 (1 mm ×1 mm) computational mesh is implemented between the contacts. As shown in Fig. 4, the simulated average peak velocity reaches up to 9.8×10^7 cm/s and the corresponding risetime can be estimated about 1.0 ns. At later times, the drift velocity is of the order of 10^7 cm/s as most of the electrons reach the satellite valleys.

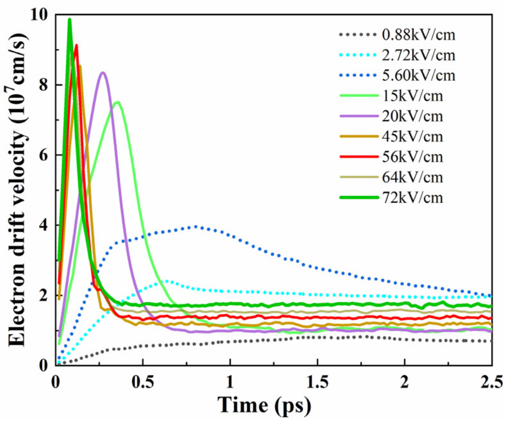

Fig. 4. The simulated average drift velocity of single-shot operation with respect to different bias electric fields.

Furthermore, considering the nJ optical excitation, the induced changes in absorption also arise from the increase of bias electric field and the internal temperature due to the joule heat. A simplified formula of the Franz-Keldysh (F-K) effect as follows [13]:

$$\alpha \propto \exp\{-[4\sqrt{2m^*}(E_g - \hbar\omega)^{3/2}]3eEh\} \tag{5}$$

where α is the absorption coefficient, m^* is the electron effective mass, e is the electron charge, E_g is the band gap energy, E is the bias electric field, and the $\hbar\omega$ is the photon energy. It can be calculated that a field of ~50 kV/cm is equivalent to a 10 meV decrease in the energy band gap. Therefore, the change of absorption edge in higher electric field also can lead to the variation of photogenerated carriers' amount in higher electric field. Consequently, a more drastic carriers' dynamic process is induced which is in form of an enhanced carriers' avalanche multiplication process.

C. 1-kHz HG characteristics at 80 kV/cm

In linear operation with relative weak avalanche multiplication of carrier, GaAs PCSS can be easily operated up to 80 MHz without breakdown as the optical excitation is of tens nJ. Although the repetitive HG operation has been achieved by laser diode arrays in µJ regime [7] [14], the PCSS lifetime still has the limitation. For example, it will need 100 µJ to yield 2 kA for 20 ns without PCSS breakdown, in which 100 filaments will be produced and a more complicated optical delivery system is required [14]. The significant reduction in lifetime is the constraint for GaAs PCSS in practical applications as each filament current increases above 30 A [15]. Despite the benefits of high current or voltage, the switch longevity is restricted fundamentally by long duration time that leads to the unfavorable electric field distortion and thermal runaway [16].

In our experiment, it is not carried out to pursue the extreme lifetime of HG GaAs PCSS, but rather to study the characteristics for the purpose of avoiding the device instabilities, especially at nJ optical excitation. Practically, the degradation and damage at the anode contact is more severe than at the cathode even though the current density is similar [17]. As shown in Fig. 5(a), the superposed waveforms are obtained at 1 kHz in room temperature, while the incident optical spot is centered on GaAs and the PCSS is biased at 80 kV/cm. The transients are attenuated by 60 dB and the reproducibility of the waveforms is excellent. Results show that the degradations almost arose nearby the anode as the extreme conditions are attempted in our experiment. Moreover, the location of the incident laser spot between the opposite contacts, also plays an important role on the device performance at single-shot and continuous operation. The experimental results have proved that the repetitive operation is more stable while the cathode plane is excited, and the laser spot is in the center of gap.

According to the electrode gap size (1 mm) and the electron velocity at high electric field (~10^8 cm/s) [8], [18], the transit time can be estimated to about 1 ns, which coincides very closely with the experimental average risetime

(1.04ns). Considering the optical excitation energy, the initial concentration of photogenerated carriers is relatively low. Due to the high bias electric field of 80 kV/cm, the electrons' impact ionization dominates the photoconduction and the carriers' concentration increases drastically. The photogenerated carriers start to transit from cathode to anode in the form of electron domains. Certainly, the heat effect is important for the continuous or repetitive PCSS operation circumstance while the thermal issue can be ignored at the single-shot operation.

The joule heat dQ deposited into a unit volume (V) during transient time dt can be approximated by:

$$dQ = JEV \cdot dt \tag{6}$$

where J is the current density the and E is the electric field. Assuming all the joule heat dQ transforms into heat energy in filamentary channel without heat loss. Then, the incremental temperature dT can be expressed by:

$$dQ = \rho_m C_p V \cdot dT \tag{7}$$

where ρ_m is the mass density of GaAs and C_p is the specific heat. Combining Eq. (6) and Eq. (7), the incremental temperature ΔT for a confined region can be written by:

$$\Delta T = \int \frac{JE}{\rho_m C_p} dt = \int \frac{q \mu n E^2}{\rho_m C_p} dt \tag{8}$$

where q is the electric charge, μ and n are the photogenerated carriers' mobility and density, respectively. Equation (8) indicates that the increase of temperature in PCSS is directly proportional to the density of photo-generated carriers and the square of the electric field. Note that, the adiabatic assumption is considered during this heating process. The thermal accumulation will influence eventually the performance of GaAs PCSS and melt the electrodes at a certain continues operation time. Therefore, it is necessary to evaluate the electric field distribution, especially for the repetitive operation.

The temporal evolution of the internal electric field at 140 nJ excitation can be demonstrated by the EMC simulation developed in the previous section. The three-valley Γ-L-X model of conduction band structure is employed. As addressing the Poisson equation, the real photogenerated carriers is conceived as an ensemble of 2×10^4 super-particles, in which the charge depends on the excitation energy and varies with the photogenerated carriers' density . The transient electric field distribution at 1ns is plotted in Fig. 5(b). It demonstrates that the transient electric field in the vicinity of the anode is enhanced dramatically and up to ~174 kV/cm. The simulated result is verified that the electric field strength closing to the anode becomes higher than other area in the gap. In this regard, one can estimate approximately the total temperature rise with joule heating for the time scales of interest, in which the repetition rate should also be considered. The longer the switching pulse duration time or the higher repetition rate, the bigger temperature increment. Eventually, it is predictable that the electrode shedding or thermal breakdown will occur, if the temperature reaches at the melting point of the alloy electrodes and GaAs wafer.

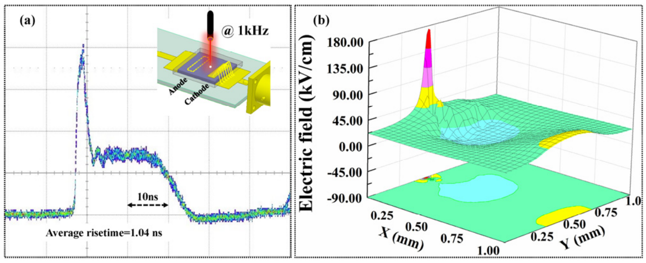

Fig.5. (a)1-kHz repetitive superposed waveforms at 80 kV/cm (Y/div 1V, X/div 10 ns), attenuated by 60 dB. The average risetime is about 1.04ns. The inset is the trigger sketch of PCSS (b) Transient electric field distribution at the time=1 ns for pulsed optical excitation with 9 ns FWHM centered at t=0. X is the direction from anode to cathode and Y is direction parallel to the contacts.

IV. CONCLUSION

In summary, the transient HG operation of GaAs PCSS with opposed contacts is performed under LD triggering. The contacts are made with Ni/AuGe/WTi/Au alloy while the WTi is served as the diffusion block layer to enhance the device stability at repetitive operation. The electric field dependence of carriers' avalanche multiplication factor and risetime are obtained as the optical excitation is fixed at 140 nJ. The effect of electric field on the photogenerated carriers' dynamic process and the thermal accumulation at repetition rate is analyzed. The stable 1kHz HG operation is achieved at 80 kV/cm and the maximum avalanche multiplication factor reaches up to 0.8×10^4.The transient electric field distribution is illustrated by an ensemble Monte Carlo simulation, which reveals that the anode protection is of great importance. Moreover, it constitutes a future advance for kHz repetitive operation of HG GaAs PCSS at nJ optical excitation.

REFERENCES

[1] Long Hu, Jiancang Su, Ruicheng Qiu, Xu Fang, and Jingxuan Wang, "Failure mechanism of a low-energy-triggered bulk gallium arsenide avalanche semiconductor switch: simulated analysis and experimental results," *IEEE Transactions on Electron Devices*, vol. 65, no. 9, pp. 3855-3861, Sept. 2018. DOI: 10.1109/TED.2018.2859231

[2] Langning Wang, and Jingliang Liu, "Solid-state nanosecond pulse generator using photoconductive semiconductor switch and helical pulse forming line," *IEEE Trans. Plasma Sci.*, vol. 45, no. 12, pp. 3240-3245, Dec. 2017. DOI: 10.1109/TPS.2017.2764502

[3] Ming Xu, Mengxia Li, Wei Shi, Cheng Ma, Qin Zhang, Linlin Fan, Xiaoyan Shang, and Pengbo Xue, "Temperature-dependence of high-gain operation in GaAs photoconductive semiconductor switch at 1.6 µJ excitation," *IEEE Electron Device Letters*, vol. 37, no. 1, pp. 67-70, Jan. 2016. DOI: 10.1109/LED.2015.2503298

[4] G. M. Loubriel, Fred J. Zutavern, Alan Mar, Harold P. Hjalmarson, Albert G. Baca, Martin W. O'Malley, Wesley D. Helegeson, R. Aaron Falk, and Darwin J. Brown, "Longevity of optically activated, high gain GaAs photoconductive semiconductor switches," *IEEE Trans. Plasma Sci.*, vol. 26, no. 5, pp.1393–1402, Oct. 1998. DOI: 10.1109/27.736024

[5] W. C. Nunnally, "Critical component requirements for compact pulse power system architectures," *IEEE Trans. Plasma Sci.*, vol. 33, no. 4, pp. 1262–1267, Aug. 2005. DOI: 10.1109/TPS.2005.852406

[6] Chongbiao Luan and Hongtao Li, "Influence of hot-carriers on the on-state resistance in Si and GaAs photoconductive semiconductor switches working at long pulse width," Chin. Phys. Lett. **37** (4), 044203 (2020). DOI: 10.1088/0256-307X/37/4/044203

[7] Fred J. Zutavern, Steven F. Glover, Kim W. Reed, Michael J. Cich, Alan Mar, Michael E. Swalby, Terese A. Saiz, Michael L. Horry, Fred R. Grunner, and Forest E. White, "Fiber-optically controlled pulsed power

switches” IEEE Trans. Plasma Sci. **36** (5),2553 (2008). DOI: 10.1109/TPS.2008.2004367

[8] G. M. Loubriel, F. J. Zutavern, H. P. Hjalmarson, R. R. Gallegos, W. D. Helgeson, and M. W. O’Malley, “Measurement of the velocity of current filaments in optically triggered, high gain GaAs switches,” Appl. Phys. Lett., **64**, 3323 (1994). DOI: 10.1063/1.111266

[9] Ming Xu, Rujun Liu, Xiaoyan Shang, Qin Zhang, Wei Shi, and Gaoyuan Guo, “High-gain operation of GaAs photoconductive semiconductor switch at 24.3 nJ excitation,” *IEEE Electron Device Letters*, vol. 37, no. 6, pp. 751-753, June. 2016. DOI: 10.1109/LED.2016.2556858

[10] Bjorn Vermeersch, Gilles Pernot, Hong Lu, Je-hyeong Bahk, Art Gossard, and Ali Shakouri, “Picosecond joule heating in photoconductive switch electrodes,” *Physical Review B*. **88**, 1136-1138 (2013). DOI: 2010.1103/PhysRevB.88.214302

[11] Long Hu, Jiancang Su, Zhenjie Ding, and Qingsong Hao, “A low-energy-triggered bulk gallium arsenide avalanche semiconductor switch with delayed breakdown,” *IEEE Electron Device Lett.,* vol. **36**, no. 11, pp. 1176-1179 (2015). DOI: 10.1109/LED.2015.2475698

[12] Liangxiu Ye, *Semiconductor Physics,* Beijing, China: Higher Education Press, 2009, pp. 192-193

[13] K. Seeger, *Semiconductor Physics: an introduction*. Berlin, Germany: Springer-Verlag, 345-346 (1999).

[14] Fred J. Zutavern, Guillermo M. Loubriel, Harold P. Hjalmarson, Alan Mar, Wesley D. Helgeson, Martin W. O’Malley, Mitchell H. Ruebush, “Properties of high gain GaAs switches for pulsed power applications”, in *11th IEEE Pulsed Power Conference*, Baltimore, vol. 2, pp. 959-964 (1997). DOI: 10.1109/PPC.1997.674517

[15] Alan Mar, Guillermo M. Lourbriel, Fred J. Zutavern, Martin W. O’Malley, Wesley D. Helgeson, Darwin J. Brown, Harold P. Hjalmarson, Albert G. Baca, R. L. Thornton and R. D. Donaldson, “Doped contacts for high-longevity optically activated, high-gain GaAs photoconductive semiconductor switches”, *IEEE Transactions on Plasma Science*, vol. 28, no. 5, pp. 1507-1511 (2000). DOI: 10.1109/27.901223

[16] Animesh R. Chowdhury, Richard Ness, and Ravi P. Joshi, “Assessing lock-on physics in semi-insulating GaAs and InP photoconductive switches triggered by subbandgap excitation,” *IEEE Transactions on Electron Devices*, vol. 65, no.9, pp. 3922-3929 (2018). DOI: 10.1109/TED.2018.2856803

[17] Yi Shen, Yi Liu, Wei Wang, Mao Ye, Huang Zhang, and Liansheng Xia, “Anode failure mechnism of GaAs photoconductive semiconductor switch triggered by laser diode”, *IEEE Transactions on Plasma Science*, vol. 47, no.10, pp. 4584-4587 (2019). DOI: 10.1109/TPS.2019.2906696

[18] Fred J. Zutavern, Albert G. Baca, Weng W. Chow, Michael J. Hafich, Harold P. Hjalmarson, Guillermo M. Loubriel, Alan Mar, Martin W. O’Malley, L. D. Roose, and G. Allen Vawter, “Electron-hole plasmas in semiconductors”, in *28th IEEE ICOPS*, Las Vegas, vol.1, pp. 289-293 (2001). DOI: 10.1109/PPPS.2001.1002049